Brain BOLD and NIRS response to hyperoxic challenge in sickle cell disease and chronic anemias

Chau Vu, Adam Bush, Matthew Borzage, Soyoung Choi, Julie Coloigner, Shayan Farzad, Yaqiong Chai, Thomas Coates, John Wood

Brain BOLD and NIRS response to hyperoxic challenge in sickle cell disease and chronic anemias

Chau Vu,[1] Adam Bush,[1,2] Matthew Borzage,[3,4] Soyoung Choi,[5] Julie Coloigner,[6,7] Shayan Farzad,[1] Yaqiong Chai,[1] Thomas D. Coates,[8,9] John C. Wood[2,10]

[1]Department of Biomedical Engineering, University of Southern California, Los Angeles, CA
[2]Department of Radiology, Stanford University, Stanford, CA
[3]Division of Neonatology, Fetal and Neonatal Institute, Children's Hospital Los Angeles, Los Angeles, CA
[4]Department of Pediatrics, Keck School of Medicine, University of Southern California, Los Angeles, CA
[5]Neuroscience Graduate Program, University of Southern California, Los Angeles, CA
[6]CIBORG Laboratory, Division of Radiology, Children's Hospital Los Angeles, Los Angeles, CA
[7]Univ Rennes, CNRS, Inria, Inserm, IRISA UMR 6074, Empenn ERL U 1228, F-35000 Rennes, France
[8]Division of Hematology-Oncology, Department of Pediatrics, Children's Hospital Los Angeles, Los Angeles, CA
[9]Departments of Pediatrics and Pathology, Keck School of Medicine, University of Southern California, Los Angeles, CA
[10]Division of Cardiology, Departments of Pediatrics and Radiology, Children's Hospital Los Angeles, Los Angeles, CA

Abstract:

Purpose: Congenital anemias, including sickle cell anemia and thalassemia, are associated with cerebral tissue hypoxia and heightened stroke risks. Recent works in sickle cell disease mouse models have suggested that hyperoxia respiratory challenges can identify regions of the brain having chronic tissue hypoxia. Therefore, this work investigated differences in hyperoxic response and regional cerebral oxygenation between anemic and healthy subjects.

Methods: A cohort of 38 sickle cell disease subjects (age 22 ± 8 years, female 39%), 25 non-sickle anemic subjects (age 25 ± 11 years, female 52%), and 31 healthy controls (age 25 ± 10 years, female 68%) were examined. A hyperoxic gas challenge was performed with concurrent acquisition of blood oxygen level-dependent (BOLD) MRI and near-infrared spectroscopy (NIRS). In addition to hyperoxia-induced changes in BOLD and NIRS, global measurements of cerebral blood flow, oxygen delivery, and cerebral metabolic rate of oxygen were obtained and compared between the three groups.

Results: Regional BOLD changes were not able to identify brain regions of flow limitation in chronically anemic patients. Higher blood oxygen content and tissue oxygenation were observed during hyperoxia gas challenge. Both control and anemic groups demonstrated lower blood flow, oxygen delivery, and metabolic rate compared to baseline, but the oxygen metabolism in anemic subjects were abnormally low during hyperoxic exposure.

Conclusion: These results indicated that hyperoxic respiratory challenge could not be used to identify chronically ischemic brain. Furthermore, the low hyperoxia-induced metabolic rate suggested potential negative effects of prolonged oxygen therapy and required further studies to evaluate the risk for hyperoxia-induced oxygen toxicity and cerebral dysfunction.

Introduction:

Congenital anemias, including sickle cell anemia and thalassemia, are some of the most common monogenic disorders in the world and lead to an array of clinical manifestations in many organ systems.[1] In the brain, chronic anemia is associated with compensatory increases in cerebral blood flow to preserve global brain oxygen delivery.[2,3] However, this compensatory cerebral hyperemia is maldistributed, leaving deep watershed areas hypoxic[4,5] and prone to increased stroke risk[6–9], while the cerebral cortex is spared. Recent work using MRI tissue oximetry and arterial spin labeling demonstrate that these areas have inadequate oxygen delivery,[10] increased oxygen extraction fraction (OEF)[11] and impaired vasodilatory reserve.[12] Consequently, there is significant shrinkage of the deep white matter, while cortical thickness is preserved.[13–15]

In sickle cell disease (SCD) mouse models, the use of 100% oxygen gas challenge has been shown to identify chronically hypoxic brain regions.[16] The hyperoxic ventilation increases arterial oxygen content by approximately 1.1 ml O_2/ml blood through increases in dissolved oxygen concentration. Although this is a modest effect in healthy non-anemic subjects, this addition would increase oxygen content by approximately 10% in anemic patients of hemoglobin of 7 g/dl. We postulated that the increased O_2 capacity with 100% oxygen supplementation could be beneficial in the deep white matter where compensatory hyperemia is blunted. Furthermore, we anticipated that deep white matter structures would exhibit greater improvements in oxygen saturation compared with the cerebral cortex.

Therefore, to investigate for possible regional cerebral oxygen delivery impairment, we performed a hyperoxia challenge and used non-invasive near-infrared spectroscopy (NIRS) and Blood-Oxygen-Level-Dependent (BOLD) MRI acquisitions to measure hyperoxic responses in a cohort of healthy volunteers, patients with sickle cell anemia, and patients with non-sickle anemia. We hypothesized that hyperoxia would reveal brain regions with pathologic flow limitations and elevated peak extraction at baseline conditions by way of greater increase in BOLD signal compared to adequately perfused, healthy tissue. We augmented this analysis with measurements of global oxygen delivery and metabolism under baseline and hyperoxic conditions to further shed light on the supply-demand mismatch and the brain's compensation mechanism for the decreased oxygen carrying capacity in SCD and other anemias.

Methods:

Study population:

All studies were performed at Children's Hospital Los Angeles and approved by the Committee on Clinical Investigation (CCI#2011-0083). Informed consent or assent was obtained from all study participants. This study was performed in accordance with the Declaration of Helsinki of 1975. A total of 94 subjects were tested between April 2012 and February 2018. Only subjects older than 12 years of age were included in the study because of the challenge of complying with the respiratory apparatus. Imaging, vital signs and blood samples were obtained on the same day for each subject.

The first group consisted of 38 SCD subjects: 34 subjects with SS hemoglobin and four subjects with SC hemoglobin. Exclusion criteria were prior overt stroke, pregnancy, acute chest or pain crisis hospitalization within one month and major medical problems outside of their chronic anemia. Asymptomatic iron overload was permitted. Out of 38 SCD subjects, 15 patients were receiving blood transfusions every three to four weeks to lower their hemoglobin S percentage to below 30%. Of the remaining 23 SCD patients, 15 were receiving hydroxyurea with good MCV and hemoglobin F response.

The second group of anemic control (ACTL) subjects consisted of 25 individuals with non-sickle chronic anemia. This group was not race-matched to the SCD group, with eleven subjects with β thalassemia major, two subjects with thalassemia intermedia, three subjects with Eβ thalassemia, one subject with autoimmune hemolytic anemia, one subject with aplastic anemia,

three subjects with hemoglobin H constant spring, one subject with congenital dyserythropoietic anemia and three subjects with hereditary spherocytosis. Patients were excluded if they had any chronic organ dysfunction such as diabetes, abnormal renal function, or chronic active hepatitis. Asymptomatic iron overload was permitted. The three patients with spherocytosis had been splenectomized and had supranormal hemoglobin levels. Fifteen out of 25 ACTL subjects were receiving blood transfusions every three to four weeks. All chronically transfused patients (SCD and ACTL) were studied on the same day of their regularly scheduled blood transfusion, prior to receiving blood, when their hemoglobin levels were at the lowest. Four of the ACTL subjects had >10% hemoglobin F or fast moving hemoglobin species that exhibit high oxygen affinity.

The third group of healthy volunteers was race-matched to the SCD population, consisting of 31 African and Hispanic American controls (CTL). Subjects were excluded if they had any poorly controlled chronic illnesses such as diabetes, hypertension or hepatitis. Since most subjects in this group were first or second-degree relatives of the SCD patients, sickle cell trait was common, occurring in 16/31 of the controls; these are subjects who had approximately 40% HbS in their blood but no cells containing exclusively HbS.

Imaging and blood samples were obtained on the same day for each subject. All imaging was performed on a Philips Achieva 3T MR system with an eight-channel, receive-only head coil. Complete blood count, reticulocytes, quantitative hemoglobin electrophoresis and cell-free hemoglobin levels were analyzed in our clinical laboratory. Demographic and clinical variables of each subject group are summarized in Table 1.

Hyperoxia gas challenge:

The gas challenge setup has been previously reported[17] and is illustrated in Figure 1. At the start of the image acquisitions, patients were breathing through a two-liter reservoir rebreathing circuit supplied by pressurized, non-humidified room air at 12 liters per minute. This system included one-way valves to prevent partial gas mixtures and respiratory bellows (Invivo Corporation, Gainesville, FL) to display the breathing pattern and frequency. At 50 seconds into the data acquisition, the room air gas mixture was switched to 100% oxygen until the end of the acquisition (total oxygen duration 5.1 minutes). Peripheral arterial oxygen saturation (SpO_2) was acquired by fingertip pulse oximetry concurrently with forehead NIRS and BOLD MRI during the gas challenge.

Near-infrared spectroscopy (NIRS):

A NIRS system (NIRO-200 system, Hamamatsu Photonics, Hamamatsu City, Japan) was used to measure relative changes in oxygenated hemoglobin (OxyHb), deoxygenated hemoglobin (DeoxyHb) and tissue oxygen index (TOI) of the mixed venous-weighted blood in the cerebral circulation continuously throughout the anatomical and challenge imaging exam (Figure 1).[18] The probes were placed on the subject's forehead to record oxygenation in the watershed area between the anterior and medial cerebral arteries.[19] NIRS signals were acquired and synchronized via a Biopac MP150 data acquisition system (BioPac, Goleta, CA) oversampled at 1kHz.

NIRS measurements were recorded concurrently during the hyperoxia challenge (Figure 1). A modified Beer-Lambert law was used to calculate the relative change in OxyHb, DeoxyHb, TOI, and total hemoglobin (TotalHb, equivalent to the sum of OxyHb and DeoxyHb).

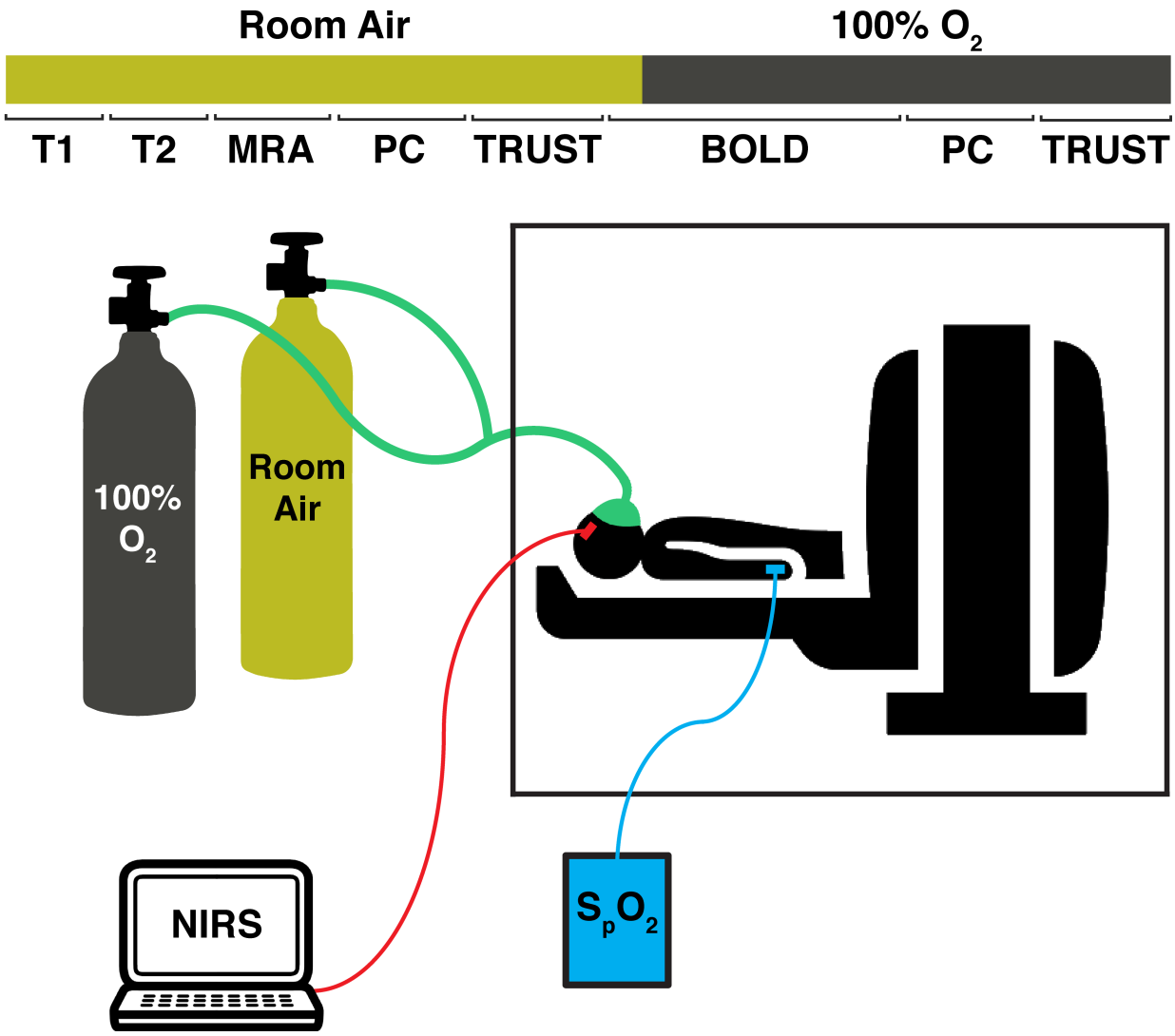

Figure 1. Experimental setup. Anatomical 3D T1 and T2-FLAIR, BOLD, T2-Relaxation-Under-Spin-Tagging (TRUST) and phase contrast scans were performed in all subjects under normoxia and hyperoxia conditions. BOLD imaging was performed under 50 seconds of normoxia and 4 minutes of hyperoxia to capture the cerebral hemodynamic response to 100% oxygen inspiration. Near-infrared spectroscopy (NIRS) and peripheral S_pO_2 were measured simultaneously with the BOLD acquisition during hyperoxia.

Magnetic resonance imaging:

Each participant underwent an MRI study using a 3T Philips Achieva with an 8-element phased-array coil. Anatomical 3D T1, T_2-Relaxation-Under-Spin-Tagging (TRUST)[20] to measure venous saturation (Y_v) and phase contrast[21] to measure global cerebral blood flow (CBF) were performed in all subjects under normoxic condition. Following the last baseline imaging sequence, the hyperoxic ventilation commenced after 50 seconds into the five-minute BOLD acquisition. After BOLD imaging, repeated TRUST and phase contrast scans under hyperoxia were performed. The sequence of all MR acquisitions is illustrated in Figure 1. All MR acquisition parameters are listed below and were identical between normoxic and hyperoxic imaging.

A 3D T1-weighted image was acquired covering the whole brain (160 sagittal slices) with TR = 8ms, TE = 4ms, flip angle = 8°, in-plane resolution = 1mm × 1mm, FOV = 256mm × 256mm and slice thickness = 1.0mm. The T2-weighted FLAIR 3D image was acquired with the following parameters: TR = 4800 msec, TE = 257.9 msec, inversion time (TI) = 1650 msec, in-plane resolution = 1 × 1 mm, FOV = 256 × 256 mm, and slice thickness = 1.3 mm. MR angiography image was acquired: TR = 23 msec, TE = 3.45 msec, flip angle = 18, FOV = 220 × 220 mm, resolution = 0.38 × 0.38 mm, and slice thickness = 1.4 mm.

To measure CBF, phase contrast MRI was obtained, positioned just above the carotid bifurcation: FOV = 260 x 260 mm, TE = 7.5ms, slice thickness = 5 mm, encoding velocity = 150 cm/s, and 10 signal averages. A VENC of 150 cm was chosen because of the increased blood velocities observed in chronically anemic subjects. To measure T2 relaxation of blood, TRUST was acquired at the superior sagittal sinus with the following parameters: CPMG T_2 preparation with effective echo times of 0, 40, 80 and 160 ms, TR = 1978 ms, delay time = 1022 ms, resolution = 3.4 × 3.4 × 5 mm and FOV = 220 × 220 × 5 mm. BOLD images were acquired using gradient-echo echo-planar-imaging sequence: TR = 2000 ms, TE = 50 ms, in-plane resolution = 2.3 × 2.3 mm, FOV = 220 × 220 mm, 26 axial slices, slice thickness = 5 mm, SENSE factor of 2. A total of 150 volumes were collected in five minutes. All MR acquisition parameters have been detailed in prior publications.[10,22,23]

T1, T2-FLAIR, and MRA angiography images were reviewed by a board certified neuroradiologist. Silent cerebral infarcts were defined according to the Silent Ischemia Trial criteria,[24] which requires a white matter hyperintensity > 3 mm in orthogonal planes.

Definitions of NIRS and BOLD changes in response to hyperoxia:

The following definitions of hypoxic parameters were provided for DeoxyHb but without loss of generality were used to compute response dynamics for OxyHb, TotalHb, TOI and BOLD time series:

(1) $\mathbf{DeoxyHb_{baseline}}$ was the mean DeoxyHb signal before hyperoxic gas, calculated from the start of the BOLD acquisition to the start of oxygen gas administration at 50 seconds.

(2) $\mathbf{DeoxyHb_{hyperoxia}}$ was the mean signal after the signal has stabilized during hyperoxia, calculated from 120 seconds to the end of the BOLD acquisition.

(3) $\Delta_{\mathbf{DeoxyHb}}$ (the depth of the hyperoxic change, *μmol* for NIRS and *%* for BOLD changes) was calculated as $\Delta_{DeoxyHb} = |DeoxyHb_{baseline} - DeoxyHb_{hyperoxia}|$.

Pictorial illustrations of these definitions can be found in Figure 2.

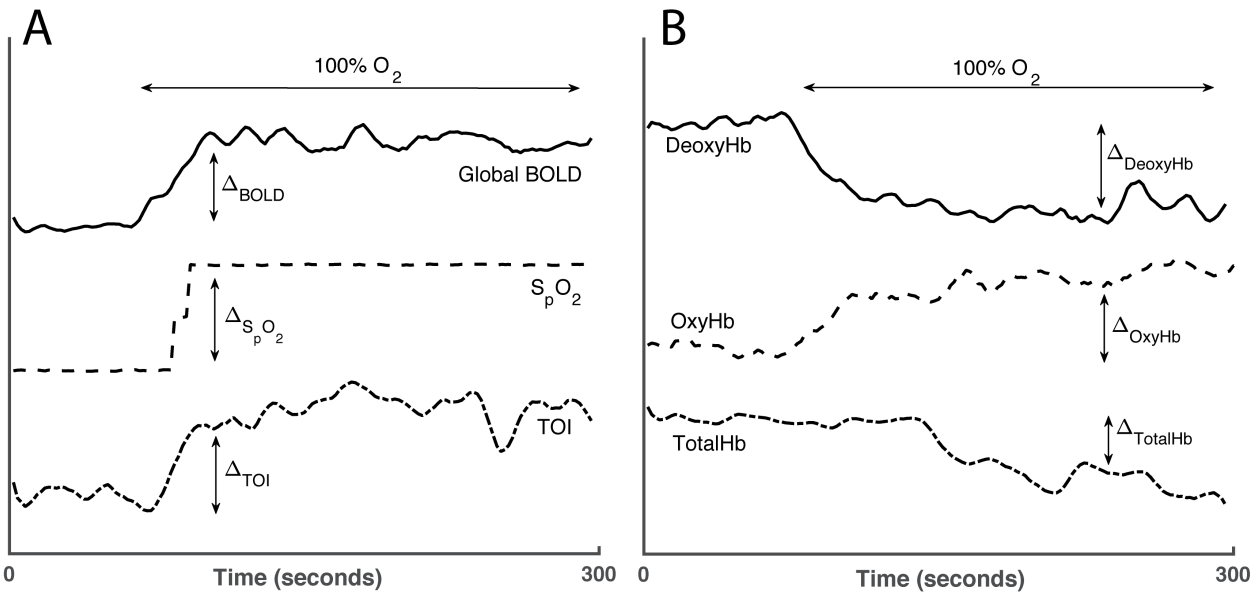

Figure 2. Sustained hyperoxia model signals. Representative recordings of (A) global BOLD, S_pO_2, tissue oxygen TOI, (B) deoxygenated hemoglobin DeoxyHb, oxygenated hemoglobin OxyHb and total hemoglobin TotalHb changes during the hyperoxia challenge.

Image processing:

Structural T1 images were registered to the Montreal Neurological Institute (MNI) template with the FMRIB Software Library (FSL); BOLD images were preprocessed with FSL and registered to MNI template space using a standard spatial functional pipeline.[23] Global Δ_{BOLD} values were computed as an average within a whole-brain mask derived from an average of 152 T1-weighted MRI scans in the common MNI coordinate system.[25] MNI-based grey matter mask, an eroded white matter mask and three vascular territories masks were used to calculate average Δ_{BOLD} for these different brain regions. Masks of the anterior cerebral artery, middle cerebral artery and posterior cerebral artery circulations were based on the published templates of vascular territories in both hemispheres.[26] The territories were created from anatomic studies of cerebral vascularization and evaluated on the bicommissural plane.

Whole-brain CBF was measured using phase contrast MRI,[21] and phase contrast images were analyzed using an in-house MATLAB program (Mathworks, Natick, MA). Stationary tissue pixels were identified in the complex difference images by simple thresholding using a mean plus two standard deviations from a remote, nonvascular region. Vessel boundaries were semi-automatically segmented from complex difference images using Canny edge detection and mapped to the phase difference image for flow calculation. Total CBF, which was the sum of the flow in left and right interior carotid arteries and vertebral arteries, was corrected for brain size assuming a brain density of 1.05 g/ml.

For the TRUST acquisition, the difference signals between tag and control images of the superior sagittal sinus cross sections were fitted to a mono-exponential decay equation $\Delta S=\Delta S_0 e^{eTE\times(1/T_{1b}-1/T_{2b})}$, where eTE = 0, 40, 80 and 160ms, T_{1b} and T_{2b} are the relaxation parameters of blood. T_{1b} was estimated from the hematocrit in patients with normal hemoglobin or as a value of 1818ms for patients with sickle.[27] T_{2b} was derived from nonlinear least squares fit to the signal decay equation. Afterward, T_{2b} and hematocrit were used to estimate venous saturation from a previously-published calibration curve for non-sickle[28] and SCD blood.[29]

Physiological parameters:

Several physiological parameters were derived using the following equations:

$$C_aO_2 = 1.34 \times Hb \times Y_a + 0.003 \times P_aO_2 \text{ (ml } O_2\text{/ml blood)} \quad [1]$$

$$C_vO_2 = 1.34 \times Hb \times Y_v + 0.003 \times P_vO_2 \text{ (ml } O_2\text{/ml blood)} \quad [2]$$

$$OEF = 1 - \frac{C_vO_2}{C_aO_2} \quad [3]$$

$$O_2\ delivery = CBF \times C_aO_2 \text{ (ml/100g/min)} \quad [4]$$

$$CMRO_2 = CBF \times (C_aO_2 - C_vO_2) \text{ (ml } O_2\text{/100g/min)} \quad [5]$$

where P_aO_2 is the arterial partial pressure of oxygen estimated to be 100 mmHg at normoxia and 400 mmHg at hyperoxia, P_vO_2 is the venous partial pressure of oxygen estimated to be 40 mmHg at normoxia and 52 mmHg at hyperoxia,[30] C_aO_2 is the arterial oxygen content, C_vO_2 is the venous oxygen content, *Hb* is the hemoglobin level of each subject, Y_v is the venous saturation measured by TRUST, Y_a is the arterial saturation measured by pulse oximetry and OEF is the cerebral oxygen extraction fraction.

Statistical analysis:

Statistical analysis was performed in JMP (SAS, Cary, NC). One-way ANOVA with Dunnett's post hoc correction was used to examine the difference in clinical and oxygenation variables between SCD and control, and between ACTL and control; independent samples *t*-test was used to compare SCD and ACTL groups. Univariate and stepwise multivariate regressions were performed against hemoglobin, HbS, transfusion status, fetal hemoglobin, white blood cells, platelets, reticulocytes and cell-free hemoglobin; multivariate predictors were retained in the final model for $p<0.05$. Two-sample *t*-maps were generated with Analysis Functional NeuroImages (AFNI)[31] to compare desaturation parameters between controls and SCD or ACTL patients; each voxel's *t*-statistic was calculated by $t = (\overline{x_{SCD/ACTL}} - \overline{x_{CTL}}) / (s_p \sqrt{\frac{1}{n_{SCD/ACTL}} + \frac{1}{n_{CTL}}})$, with $n_{SCD/ACTL}$ and n_{CTL} as group sizes, $\overline{x_{SCD/ACTL}}$ and $\overline{x_{CTL}}$ as parameter means, $s_{SCD/ACTL}$ and s_{CTL} as parameter standard deviations and s_p as the pooled standard deviation $s_p = \sqrt{\frac{(n_{SCD/ACTL}-1)\, s^2_{SCD/ACTL} + (n_{CTL}-1)\, s^2_{CTL}}{n_{SCD/ACTL}+n_{CTL}-2}}$. Age and sex regressions were performed in JMP, and the average was added to the regressed values to ensure final values were within physiologically meaningful range.

Results:

Demographics:

Pre- and post-hyperoxia CBF, arterial and cerebral venous saturations were recorded in all patients in this study. All patients were included in the oxygen delivery and metabolism analysis. Of the 94 participating subjects, only 76 subjects were included in the BOLD analysis; the rest were excluded due to severe subject motion or incomplete BOLD acquisition. The NIRS analysis included 21 SCD subjects, 13 ACTL subjects and 20 controls, and the rest were excluded due to sensor and data acquisition system malfunctions.

The demographics for this study population is summarized in Table 1; the results are reported separately for the Bold MRI and NIRs subcohorts. There were no differences in the demographic and hematologic data between the complete cohort presented in Table 1 and the cohort after subject exclusion in the BOLD and NIRS analyses.

Since the SCD group trended younger and had more male subjects compared to controls, all subsequent analyses were corrected for age and sex. There was no significant difference between sickle-cell trait and non-trait controls in NIRS ($p=0.74$ for Δ_{OxyHb}, $p=0.95$ for $\Delta_{DeoxyHb}$, $p=0.54$ for Δ_{TOI}), global Δ_{BOLD} ($p=0.52$), CBF ($p=0.76$), or $CMRO_2$ ($p=0.28$). Thus, trait and non-trait control data was pooled.

Table 1. Patient demographic and hematologic data. Bold letterings indicate statistical significance ($p<0.05$).

Cohort with valid BOLD results

	CTL (N = 28)	SCD (N = 31)	ACTL (N = 18)	*p*-value (SCD vs. CTL)	*p*-value (ACTL vs. CTL)	*p*-value (SCD vs. ACTL)
Age (Years)	25.4 ± 10.3	22.3 ± 7.7	26.9 ± 12.1	0.46	0.87	0.27
Sex	10M, 18F	20M, 11F	9M, 9F	**0.04**	0.37	0.33
Transfusion	0/28	12/31	12/18	**<0.0001**	**<0.0001**	0.079
Arterial Saturation (%)	99.4 ± 1.0	97.6 ± 1.9	98.8 ± 1.1	**<0.0001**	0.39	**0.02**
Hemoglobin Electrophoresis	14AA, 14AS	27SS, 4SC	16AA, 2AE			
Hemoglobin (g/dl)	13.6 ± 1.1	9.8 ± 1.9	10.6 ± 2.3	**<0.0001**	**<0.0001**	0.225
Hematocrit (%)	40.2 ± 3.2	27.7 ± 4.8	32.3 ± 6.0	**<0.0001**	**<0.0001**	**0.003**
White Blood Cell Count (x10^3)	5.7 ± 2.0	9.9 ± 4.8	6.9 ± 2.3	**<0.0001**	0.50	**0.001**
Platelet Count (x10^3/µl)	242 ± 53	304 ± 111	271 ± 27	**0.05**	0.60	0.50
Reticulocytes (%)	1.4 ± 0.6	9.9 ± 5.3	2.3 ± 2.8	**<0.0001**	0.69	**<0.0001**
S-cells Fraction (%)	0	52.0 ± 31.0	0	**<0.0001**	1.00	**<0.0001**
Fetal Hemoglobin (%)	0.5 ± 2.2	7.6 ± 8.8	1.8 ± 3.6	**<0.0001**	0.78	**0.004**
Cell-free Hemoglobin (%)	6.7 ± 5.3	21.4 ± 20.6	17.8 ± 22.0	**0.004**	0.09	0.76
Cohort with valid NIRS results						
	CTL (N = 20)	SCD (N = 20)	ACTL (N = 13)	*p*-value (SCD vs. CTL)	*p*-value (ACTL vs. CTL)	*p*-value (SCD vs. ACTL)
Age (Years)	26.8 ± 10.7	23.7 ± 8.8	23.4 ± 6.8	0.54	0.55	1.0
Sex	6M, 14F	12M, 8F	6M, 7F	0.11	0.47	0.49
Transfusion	0/20	10/20	9/13	**0.0004**	**<0.0001**	0.31
Arterial Saturation (%)	99.4 ± 0.9	97.3 ± 2.1	99.1 ± 1.0	**0.0002**	0.87	**0.0045**
Hemoglobin Electrophoresis	11AA, 9AS	18SS, 2SC	11AA, 2AE			
Hemoglobin (g/dl)	13.5 ± 1.1	9.5 ± 1.8	10.6 ± 2.4	**<0.0001**	**<0.0001**	0.19
Hematocrit (%)	39.8 ± 3.1	27.5 ± 4.7	32.3 ± 5.9	**<0.0001**	**<0.0001**	**0.01**
White Blood Cell Count (x10^3)	5.5 ± 1.9	10.2 ± 4.7	7.5 ± 1.9	**<0.0001**	0.053	0.22
Platelet Count (x10^3/µl)	236 ± 54	275 ± 93	275 ± 126	0.36	0.38	0.99
Reticulocytes (%)	1.4 ± 0.7	10.6 ± 5.6	3.7 ± 3.2	**<0.0001**	0.62	**<0.0001**

S-cells Fraction (%)	0.0 ± 0.0	46.8 ± 4.7	0.0 ± 0.0	**<0.0001**	1.0	**<0.0001**
Fetal Hemoglobin (%)	0.8 ± 2.6	5.4 ± 7.2	2.2 ± 4.2	**0.02**	0.70	0.21
Cell-free Hemoglobin (%)	6.4 ± 4.2	21.8 ± 24.3	20.5 ± 24.6	**0.04**	0.98	0.11

Hematologic markers:

The SCD and ACTL groups had significantly lower hemoglobin levels (p<0.01), lower hematocrit (p<0.01) and higher cell-free hemoglobin (p<0.01) compared to healthy controls. Within the two groups of anemic subjects, SCD patients had higher reticulocytes (p<0.01), white blood cells count (p<0.01), fetal hemoglobin (p<0.01) and fraction of S-cells (p<0.01). Of all the participating ACTL subjects, 60% subjects were transfused whereas only 40% of SCD patients received regular transfusion; the transfused SCD subjects had a median HbS percentage of 19.7%, significantly lower than 76.8% in the non-transfused subgroup. Pulse oximetry values were lower in the SCD patients than control subjects at baseline (p<0.01).

Clinical imaging:

Based on MR angiography, one SCD patient had severe bilateral anterior cerebral artery stenosis, but no evidence of Moya-Moya disease. All of the other angiograms were completely normal in all three populations. None of the subjects had history of stroke, but T2-FLAIR imaging demonstrated silent cerebral infarcts in 19/38 SCD patients and 8/25 ACTL patients, compared to 7/31 control patients (p=0.04).

NIRS and BOLD response to hyperoxia:

Based on the difference in silent stroke rate between anemic and healthy subjects, oxygenation imaging was performed to shed light on the oxygen supply and demand mismatch in ischemia-prone cerebral regions. During the respiratory challenge, none of the patients consciously perceived the hyperoxia episode, and no complications were encountered. The gas challenge produced a maximum S_pO_2 values of 100%. Compared to ΔS_pO_2 in healthy controls (1.1±0.7%), ΔS_pO_2 was greater in SCD (2.4±1.6%, p<0.01) and in ACTL subjects (1.8±0.7%, p=0.06). This translated to increases in O_2 content of 1.1, 1.2, and 1.2 ml O_2/ml blood for control, ACTL, and SCD respectively.

Hyperoxia significantly increased the OxyHb concentration (p<0.01) and tissue oxygenation index (p<0.01) in the entire cohort, while DeoxyHb and total hemoglobin level decreased (both p<0.01). A summary of NIRS signal changes in each subject group is shown in Table 2. SCD subjects showed larger magnitude of change in OxyHb (p=0.01) and TOI (p<0.01) compared to controls, but there was no significant difference in the hyperoxic effect on TotalHb between the three groups (p=0.95). All NIRS changes were correlated with ΔS_pO_2 (r^2=0.14, p<0.01 for OxyHb; r^2=0.09, p=0.03 for OxyHb; r^2=0.12, p<0.01 for TotalHb; r^2=0.07, p=0.06 for TOI).

In addition to the NIRS signal, global BOLD signal was significantly increased during hyperoxic ventilation (p<0.01) and correlated with ΔS_pO_2 (Figure 3A). Global and regional Δ_{BOLD} trended higher in SCD subjects compared to healthy controls, but the difference was not statistically significant (Table 2). Additionally, Δ_{BOLD} was correlated with changes in tissue oxygenation, with 26% of the variation in Δ_{BOLD} explained by TOI (Figure 3B). The BOLD signal varied with both Δ_{OxyHb} and $\Delta_{DeoxyHb}$ (Figure 3C and 3D). Even though global Δ_{BOLD} was not correlated with total hemoglobin level (p=0.38), grey matter Δ_{BOLD} had a significant association with TotalHb (r^2=0.10, p=0.02), whereas white matter Δ_{BOLD} did not (p=0.07).

Overall, grey matter displayed a change of 3.5±1.5% in the BOLD signal in response to hyperoxic ventilation, significantly larger compared to 1.1±0.9% in the white matter (p<0.01). This pronounced grey-white matter differentiation is demonstrated by the group average Δ_{BOLD} maps in Figure 4A. Deep white matter structures did not demonstrate a different hyperoxic effect compared to gyral or more superficial white matter, and there was no significant difference in Δ_{BOLD} within the anterior, middle and posterior cerebral artery perfusion territories (p=0.14). Voxelwise comparison of Δ_{BOLD} between SCD and ACTL subjects and control subjects failed to identify any systematic differences after correction for multiple comparisons.

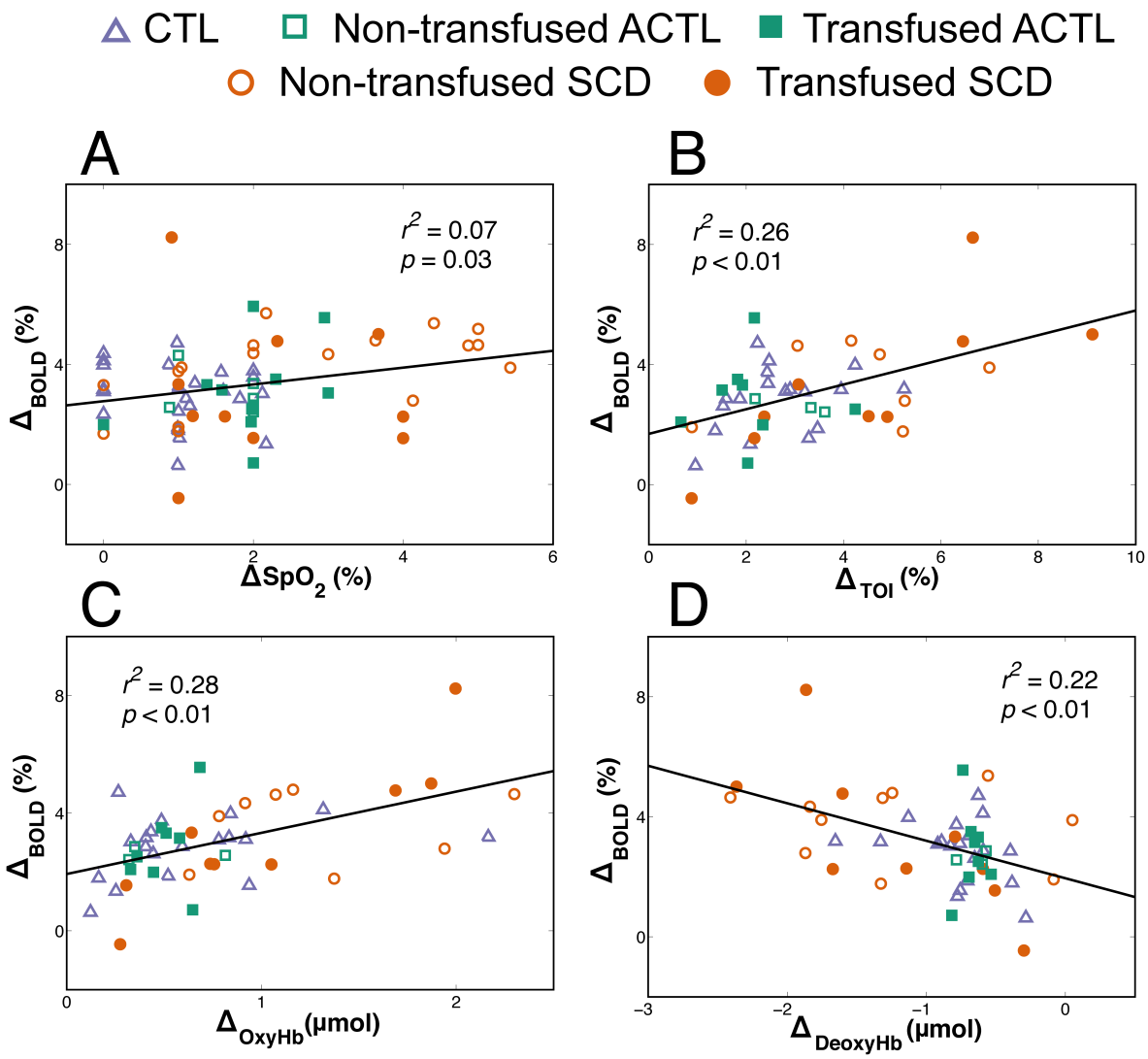

Figure 3. Correlation between changes in BOLD, NIRS and pulse oximetry signals. Correlation between Δ_{BOLD} and (A) pulse oximetry ΔS_pO_2, (B) tissue oxygenation Δ_{TOI}, (C) oxygenated hemoglobin Δ_{OxyHb}, and (D) deoxygenated hemoglobin $\Delta_{DeoxyHb}$.

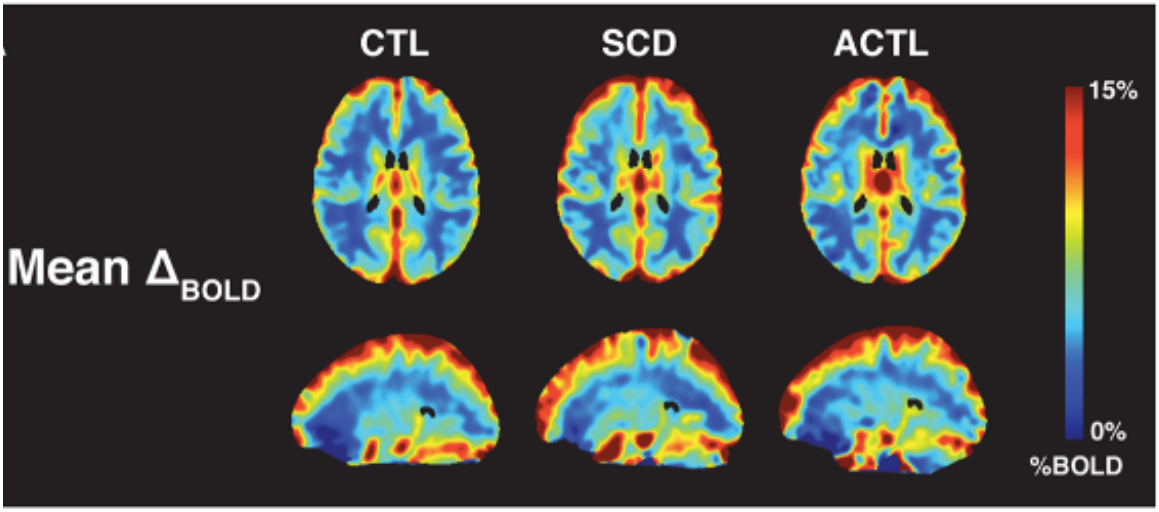

Figure 4. Group Δ_{BOLD} response to hyperoxic ventilation for sickle cell disease (SCD), non-sickle anemic (ACTL) and healthy controls (CTL). Mean Δ_{BOLD} maps for each group. T-scores between SCD and ACTL groups versus control subjects failed to identify any systematically different regional behavior (not shown).

Table 2. Group average of whole-brain and regional BOLD and NIRS changes due to hyperoxic ventilation. Bold letterings indicate statistical significance (p<0.05). GM = grey matter; WM = white matter; ACA = anterior cerebral artery territory; MCA = middle cerebral artery territory; PCA = posterior cerebral artery territory.

	CTL	SCD	ACTL	*p*-value (SCD vs. CTL)	*p*-value (ACTL vs. CTL)	*p*-value (SCD vs. ACTL)
$\Delta_{DeoxyHb}$ (µmol)	–0.83 ± 0.27	–1.10 ± 0.62	–0.64 ± 0.25	0.10	0.41	**<0.01**
Δ_{OxyHb} (µmol)	0.67 ± 0.44	1.08 ± 0.56	0.48 ± 0.21	**0.01**	0.40	**<0.01**
$\Delta_{TotalHb}$ (µmol)	–0.15 ± 0.33	–0.19 ± 0.44	–0.16 ± 0.15	0.93	0.99	0.84
Δ_{TOI} (%)	2.7 ± 1.1	4.3 ± 2.2	2.3 ± 1.0	**<0.01**	0.70	**<0.01**
Global Δ_{BOLD} (%)	3.0 ± 1.0	3.6 ± 1.7	3.1 ± 1.2	0.22	0.96	0.26
GM Δ_{BOLD} (%)	3.3 ± 1.1	3.7 ± 1.7	3.6 ± 1.5	0.58	0.77	0.87
WM Δ_{BOLD} (%)	1.0 ± 0.6	1.2 ± 1.0	1.1 ± 1.0	0.53	0.85	0.71
ACA Δ_{BOLD} (%)	3.9 ± 1.4	3.5 ± 2.3	3.7 ± 1.8	0.57	0.90	0.68
MCA Δ_{BOLD} (%)	3.7 ± 1.3	4.1 ± 1.9	3.7 ± 1.3	0.62	0.99	0.45
PCA Δ_{BOLD} (%)	4.0 ± 1.5	4.3 ± 1.9	4.8 ± 3.8	0.77	0.39	0.50

Oxygenation parameters at baseline and in response to hyperoxia:

Table 3 compares oxygen content, CBF, oxygen delivery, and cerebral metabolic rate across the patient groups at baseline and in response to hyperoxia. Arterial and sagittal sinus oxygen contents are significantly lower in both ACTL and SCD subjects compared with controls under both conditions (p<0.01 for all), but not different between them (p=0.05). There is corresponding cerebral hyperemia in both anemia groups, but to a greater extent in the SCD subjects (p<0.01); this difference did not retain significance under hyperoxia (p=0.08). Importantly, oxygen delivery was identical among all three groups under both conditions (p=0.20 for normoxia and p=0.58 for hyperoxia). OEF was lower in the anemic cohorts under both conditions (p<0.01 for both) and significantly lower in SCD subjects (p=0.02). OEF and CBF were reciprocally related to one another (r^2=0.36 room air, r^2=0.32 hyperoxia). $CMRO_2$ was also decreased in the anemic subjects compared with control subjects under both conditions (p<0.01 for both), proportional to anemia severity (r^2=0.20, p<0.01 for normoxia; r^2=0.07, p=0.01 for hyperoxia).

Table 3. Table of oxygen supply and utilization parameters under normoxia and hyperoxia. Values are expressed as mean ± standard deviation. Analysis of variance was performed with post-hoc correction using Tukey-Kramer honestly significant differences. Bold lettering depicts significant differences (p<0.05) with respect to control subjects; p-value comparing the two anemic groups is shown the rightmost column with significant values in italics.

Normoxia	**CTL**	**ACTL**	***SCD***	**p-value (ACTL vs SCD)**
Arterial O_2 Content (ml O_2/ml)	18.4 ± 1.7	**14.4 ± 3.6**	**13.0 ± 2.5**	*0.04*
Venous O_2 Content (ml O_2/ml)	11.6 ± 1.3	**9.8 ± 2.2**	**9.4 ± 2.0**	0.85
CBF (ml/100g/min)	62.9 ± 9.0	**83.0 ± 17.1**	**98.3 ± 26.8**	*<0.01*
O_2 Delivery (ml/100g/min)	11.5 ± 1.8	11.4 ± 1.9	12.4 ± 2.9	0.85
Oxygen Extraction Fraction (%)	36.8 ± 3.9	**31.6 ± 5.1**	**27.7 ± 5.2**	*<0.01*
$CMRO_2$ (ml O_2/100g/min)	4.2 ± 0.6	**3.6 ± 0.6**	**3.4 ± 0.9**	0.10
Hyperoxia				
Arterial O_2 Content (ml O_2/ml)	19.4 ± 1.7	**15.5 ± 3.6**	**14.2 ± 2.4**	0.06
Venous O_2 Content (ml O_2/ml)	12.4 ± 1.8	**10.3 ± 2.4**	**10.0 ± 2.1**	0.91
CBF (ml/100g/min)	50.0 ± 8.1	**62.9 ± 14.5**	**72.2 ± 22.3**	0.08
O_2 Delivery (ml/100g/min)	9.7 ± 1.6	9.4 ± 1.8	10.0 ± 2.7	0.99
Oxygen Extraction Fraction (%)	36.1 ± 5.8	**33.5 ± 6.8**	**29.5 ± 5.7**	*0.02*
$CMRO_2$ (ml O_2/100g/min)	3.5 ± 0.6	**3.1 ± 0.6**	**2.8 ± 0.6**	*<0.01*

Table 4 contrasts the absolute and relative changes across groups for all the brain metabolism parameters. Although the absolute increase in arterial oxygen content was identical across groups, the percentage increase was 43% – 67% higher in anemic subjects (p<0.01). In contrast, both the absolute increase (p=0.38) and percentage increase (p=0.63) in venous oxygen content was similar across groups. The absolute decline in CBF was greater in SCD patients (p<0.01 compared to controls). However, the percentage change in CBF was independent of disease state (p=0.08), averaging 22.1%. Since hyperoxia triggered a larger percentage reduction in CBF compared with the increase in oxygen content, cerebral oxygen delivery fell in all three cohorts (p<0.01). Neither the absolute decrease (p=0.31) nor the percentage decrease (p=0.48) in oxygen delivery were different across groups. Both the absolute and relative change in OEF trended higher in anemic subjects, however these differences did not reach statistical significance (p=0.09 for absolute and p=0.09 for relative changes). $CMRO_2$ declined in response to hyperoxia to a similar degree across all three cohorts (p=0.57).

Table 4. Absolute and relative changes between hyperoxia and normoxia conditions in cerebral oxygenation across groups. Values are expressed as mean ± standard deviation. Bold values are significant relative to control subjects at $p<0.05$.

	CTL		SCD		ACTL	
	Absolute Change	Percentage Change	Absolute Change	Percentage Change	Absolute Change	Percentage Change
Arterial O_2 Content (mlO_2/ml blood)	1.1 ± 0.2	6 ± 1 %	1.2 ± 0.2	**9 ± 3 %**	1.1 ± 0.2	**8 ± 3 %**
Venous O_2 Content (mlO_2/ml blood)	0.8 ± 1.1	7 ± 10 %	0.6 ± 0.7	7 ± 8 %	0.5 ± 0.8	5 ± 8 %
CBF (ml/100g/min)	–12.9 ± 7.6	–20 ± 10 %	**–26.1 ± 15.5**	26 ± 13 %	–20.1 ± 9.7	–24 ± 9 %
O_2 Delivery (ml/100g/min)	–1.9 ± 1.4	–16 ± 11 %	–2.4 ± 1.8	–19 ± 14 %	–2.1 ± 1.3	–18 ± 10 %
OEF (%)	–0.6 ± 5.7	–1 ± 16 %	1.8 ± 4.6	9 ± 23 %	1.9 ± 5.6	7 ± 20 %
$CMRO_2$ (mlO_2/100g/min)	–0.7 ± 0.7	–17 ± 17 %	–0.5 ± 0.6	–13 ± 18 %	–0.5 ± 0.7	–12 ± 21 %

Discussion:

The purpose of the present study was to determine whether we could use 100% oxygen as a contrast agent to identify brain regions having increased oxygen extraction secondary to flow limitation, as has successfully been performed in sickle cell mouse models.[16] We postulated that chronically hypoxic deep brain regions in the deep watershed areas[5,32–34] would demonstrate greater rise in BOLD signal than better perfused neighboring tissue. In this study, we evaluated the oxygen supply and utilization in the brain in response to four minutes of hyperoxic ventilation in chronically anemic patients and healthy controls. We observed higher BOLD signal and NIRS tissue oxygenation, in response to the increased blood oxygen content during hyperoxia. BOLD signal changes were more than 3-fold higher in grey matter than white matter, consistent with known relative differences in cerebral blood volume.[35] However, we failed to identify any systemic regional differences in BOLD signal changes within or across groups, suggesting that 100% oxygen could not be used to identify chronically ischemic brain regions.

The failure to replicate the results from the mouse model may stem from many reasons. Firstly, changes in white matter BOLD may mirror the grey matter response because white matter tissues are downstream in the cerebral perfusion chain. Thus, when grey matter vasoconstricts in response to 100% oxygen, there is an obligate parallel drop in white matter perfusion. Secondly, white matter BOLD signal changes are much weaker than grey matter changes because of the lower blood volume. Previous work has shown that tissue oxygenation improvements due to hyperoxia are small in low CBF areas such as the white matter compared to cortical regions,[36] so it is possible that the improvement to OEF in flow-limited areas was simply too small to observe in our study. Thirdly, our SCD population has significantly less severe disease than observed in sickle cell anemia mouse models, which were not receiving any disease modifying therapy[16].

Eighty percent of our study population was on transfusions or effective hydroxyurea treatment and some of the remaining untreated subjects had milder forms of SCD (SC and Sβ+). Our anemic and SCD subjects did not demonstrate any vasculopathy and were thus unlikely to have fixed flow limitations. Fourthly, mouse brain architecture is quite different from humans, lacking cortical infolding, and having significantly smaller frontal neocortices. As result, cerebrovascular regulation in response to oxygen and carbon dioxide challenges are likely to differ between mice and humans. Lastly, it is possible that flow limitations were spatially inconsistent, such that any regions of increased BOLD response were diluted by the group averaging.

The effect of supplemental oxygen therapy to increase cerebral partial pressure of oxygen was clearly observed in our NIRS measurements, with an average of 3% boost in tissue oxygenation index in the entire cohort. The larger TOI effect size observed in anemic patients reflects the proportionally larger increase in oxygen content in anemic subjects.[30] NIRS and BOLD changes with hyperoxia were correlated,[37] providing inter-modality corroboration of our results. However, in contrast to a previous hypoxic gas challenge in which the strongest correlation was observed between Δ_{BOLD} and $\Delta_{DeoxyHb}$,[38] the hyperoxic BOLD changes was best correlated with Δ_{OxyHb} demonstrating that hemoglobin saturation was the strongest influence of the BOLD signal rather than blood flow changes. In fact, $\Delta_{TotalHb}$ was inversely proportional to the BOLD signal. This observation supports the use of hyperoxia in calibrated fMRI, in which the increase arterial saturation rather than hyperemia is the main driving force of the changes in capillary and venous saturation observed on quantitative BOLD imaging.[39]

MRI and NIRS evidence of improved oxygenation was accompanied by powerful cerebral vasoconstriction. The vasoconstriction effect of hyperoxic ventilation was reflected by both decreased NIRS TotalHb signal and phase contrast CBF. The 20-25% decrease we observed was concordant with previous works[40,41] from independent groups. Hyperoxia with 100% oxygen administration has previously been shown to produce a ~3-7% decrease in end-tidal CO_2, but hypocapnia of this magnitude cannot explain a 20-25% reduction in CBF.[40,41] Therefore, the vasoconstriction in our results could be attributed mostly to hyperoxia,[42] which attenuates the effective nitric-oxide concentration and leads to an increase of reactive oxygen species in the brain.[43]

Improved oxygen content with hyperoxia was more than counterbalanced by the reduction in CBF. As a result, cerebral oxygen delivery declined an average of 17.7%. The decreased delivery contradicted several previous studies which found no significant change in oxygen delivery.[30,44,45] However, these studies had much smaller cohort sizes compared to the 94 subjects in this current work. In contrast, recent work by Bodetoft et al. has reported a significant decrease in systemic and coronary oxygen delivery of 4-11%, independent of arterial carbon dioxide pressure.[46]

Decreased oxygen delivery was associated with a parallel reduction in $CMRO_2$ during hyperoxia. This observation is concordant with other reports of lower metabolic rate in both the systemic[29,47] and cerebral circulations with hyperoxia.[48] The changes in oxygen delivery and metabolic rate were well-correlated, but it would be difficult to decipher whether the $CMRO_2$ reduction was a primary physiological response, triggering a subsequent reduction in O_2 delivery, or a secondary response to reduced oxygen delivery. However, given the rise in BOLD signal and NIRS tissue oxygenation index with hyperoxia, the former possibility seems more likely.

Despite the heterogenous patient groups and conditions, oxygen delivery was independent of the underlying oxygen carrying capacity and the study group, suggesting that this parameter is strongly regulated. $CMRO_2$ was also independent of study group, after controlling for differences in hemoglobin level as previously demonstrated.[49] The observed reciprocal relationship between OEF and CBF is a natural consequence of the tradeoff between vasomotor tone and oxygen extraction. In contrast, OEF is not regulated but varies significantly with the p50 of hemoglobin,[50] which in turn is impacted by red cell 2,3-DPG content and hemoglobin type.[33] Transfused red blood cells are deficient in 2-3 DPG, while hemoglobins F and H bind 2-3 DPG

less tightly, leading to much higher oxygen affinity. This contributes to the low OEF observed in the ACTL and SCD patient groups. Our findings are consistent with the results of Croal et al, who demonstrated a mean sagittal sinus OEF of 24% in young, hydroxyurea-treated patients with SCD, compared with 32% in matched control subjects.[51] Our work in an independent cohort suggests that much of the disparity in OEF between controls in anemic subjects can be explained by the p50 effects introduced by hemoglobins F and H.[33] However, decreased oxygen unloading also occurs from cerebral hyperemia, leading to capillary transit time heterogeneity,[52] or functional shunting.[27,53]

Hyperoxia, often in the form of 100% oxygen therapy, has traditionally been a transport and emergency room treatment for conditions related to poor oxygen delivery to vital organs, such as during stroke or myocardial infarction. However, subsequent studies demonstrating neutral or negative benefits have led to limiting oxygen therapy to the correction of hypoxia.[54–56] Considering that $CMRO_2$ is already impaired in anemia at baseline,[57] further hyperoxia-induced reduction in oxygen delivery and $CMRO_2$ observed in this study support that change in practice, although it is unclear whether similar responses would be observed in at risk tissues.

Our study had some important limitations. Since we were interested in a potentially clinically useful diagnostic, we did not attempt to "clamp" exhaled CO_2 levels. End-tidal CO_2 sensors were built into the breathing circuit, but technical difficulties prevented us from using these data. This study also assumed the blood pO_2 levels[30] instead of measuring it in individual patient using a radial arterial catheter. However, a 10% variation in pO_2 only leads to less than 1% change in oxygen delivery and $CMRO_2$ without changing our results. The use of a velocity encoding of 150 cm/s in phase contrast MRI was driven by the desire to avoid aliasing in anemic subjects but had suboptimal signal-to-noise for control subjects. Nonetheless, we documented inter-scan variability of 4.6% in control and anemic subjects in previous work,[3] providing sufficient robustness for the current comparisons. Additionally, our work only evaluated oxygen metabolism after a four-minute administration of 100% oxygen. Since vasoconstriction effects in hyperoxia has been shown to be reversible,[30,47] and oxygen toxicity does not manifest until several days under sustained oxygen therapy, further assessment of oxygen utilization is required to determine whether adaptation and normalization of $CMRO_2$ occurs under prolonged hyperoxic ventilation. Lastly, the SIT criteria for SCI was established from young children scanned on 1.5T scanners. The added sensitivity of 3T, plus the inexorable increase in cerebral microvascular disease with age leads to a high prevalence of SCI in our control population. Thus, the simple existence of SCI in our SCD population cannot be viewed as pathologic, but has to be placed into the broader context of normal aging.

In summary, this work evaluated the oxygen delivery and consumption in the brain during normoxic and hyperoxic ventilation. From our results, we were unable to identify brain regions of flow limitation in chronically anemic patients. However, we were able to demonstrate higher tissue oxygenation as well as arterial and venous oxygen content during hyperoxia. Even though chronic anemia is associated with hyperemia at baseline, this degree of vasodilation in SCD and anemic subjects was not enough to compensate for the hyperoxia-induced vasoconstriction in response to abnormally high pO_2, leading to diminished oxygen delivery and metabolic rate. Both controls and chronically anemic subjects showed proportional $CMRO_2$ decline compared to baseline, but the hyperoxic $CMRO_2$ values in SCD and non-sickle anemic subjects were abnormally low in our studies. Therefore, further work is needed to evaluate the risk of prolonged oxygen therapy, especially in anemic populations at risk for oxygen toxicity and cerebral dysfunction.

References:

1. Mentzer WC, Kan YW. Prospects for research in hematologic disorders: Sickle cell disease and thalassemia. *J Am Med Assoc*. 2001;285(5):640-642. doi:10.1001/jama.285.5.640
2. Borzage MT, Bush AM, Choi S, et al. Predictors of cerebral blood flow in patients with and without anemia. *J Appl Physiol*. 2016;120(8):976-981. doi:10.1152/JAPPLPHYSIOL.00994.2015
3. Bush AM, Borzage MT, Choi S, et al. Determinants of resting cerebral blood flow in sickle cell disease. *Am J Hematol*. 2016;91(9):912-917. doi:10.1002/AJH.24441
4. Chai Y, Bush AM, Coloigner J, et al. White matter has impaired resting oxygen delivery in sickle cell patients. *Am J Hematol*. 2019;94(4):467-474. doi:10.1002/AJH.25423
5. Fields ME, Guilliams KP, Ragan DK, et al. Regional oxygen extraction predicts border zone vulnerability to stroke in sickle cell disease. *Neurology*. 2018;90(13):e1134-e1144. doi:10.1212/WNL.0000000000005194
6. Kassim AA, Pruthi S, Day M, et al. Silent cerebral infarcts and cerebral aneurysms are prevalent in adults with sickle cell anemia. *Blood*. 2016;127(16):2038-2040. doi:10.1182/blood-2016-01-694562
7. Kaiafa G, Savopoulos C, Kanellos I, et al. Anemia and stroke: Where do we stand? *Acta Neurol Scand*. 2017;135(6):596-602. doi:10.1111/ane.12657
8. Chinawa JM, Ubesie AC, Chukwu BF, Ikefuna AN, Emodi IJ. Prevalence of hypoxemia among children with sickle cell anemia during steady state and crises: A cross-sectional study. *Niger J Clin Pract*. 2013;16(1):91-95. doi:10.4103/1119-3077.106774
9. Elsayh KI, Zahran AM, El-Abaseri TB, Mohamed AO, El-Metwally TH. Hypoxia biomarkers, oxidative stress, and circulating microparticles in pediatric patients with thalassemia in upper Egypt. *Clin Appl Thromb*. 2014;20(5):536-545. doi:10.1177/1076029612472552
10. Chai Y, Bush AM, Coloigner J, et al. White Matter Has Impaired Resting Oxygen Delivery in Sickle Cell Patients. *Am J Hematol*. 2019;94(4):467-474. doi:10.1002/ajh.25423
11. Fields ME, Guilliams KP, Ragan DK, et al. Regional oxygen extraction predicts border zone vulnerability to stroke in sickle cell disease. *Neurology*. March 2018:10.1212/WNL.0000000000005194. doi:10.1212/WNL.0000000000005194
12. Václavů L, Meynart BN, Mutsaerts HJMM, et al. Hemodynamic provocation with acetazolamide shows impaired cerebrovascular reserve in adults with sickle cell disease. *Haematologica*. 2019;104(4):690-699. doi:10.3324/haematol.2018.206094
13. Choi S, Bush AM, Borzage MT, et al. Hemoglobin and mean platelet volume predicts diffuse T1-MRI white matter volume decrease in sickle cell disease patients. *NeuroImage Clin*. 2017;15:239-246. doi:10.1016/J.NICL.2017.04.023
14. Choi S, O'Neil SH, Joshi AA, et al. Anemia predicts lower white matter volume and cognitive performance in sickle and non-sickle cell anemia syndrome. *Am J Hematol*. 2019;94(10):1055-1065. doi:10.1002/ajh.25570
15. Jonassaint CR, Varma VR, Chuang YF, et al. Lower hemoglobin is associated with poorer cognitive performance and smaller brain volume in older adults. *J Am Geriatr Soc*. 2014;62(5):972-973. doi:10.1111/jgs.12810
16. Kennan RP, Suzuka SM, Nagel RL, Fabry ME. Decreased cerebral perfusion correlates with increased BOLD hyperoxia response in transgenic mouse models of sickle cell disease. *Magn Reson Med*. 2004;51(3):525-532. doi:10.1002/mrm.20014
17. Vu C, Chai Y, Coloigner J, et al. Quantitative perfusion mapping with induced transient hypoxia using BOLD MRI. *Magn Reson Med*. 2021;85(1):168-181. doi:10.1002/mrm.28422
18. Jöbsis FF. Noninvasive, infrared monitoring of cerebral and myocardial oxygen sufficiency and circulatory parameters. *Science*. 1977;198(4323):1264-1267. http://www.ncbi.nlm.nih.gov/pubmed/929199. Accessed March 13, 2018.
19. Scheeren TWL, Schober P, Schwarte LA. Monitoring tissue oxygenation by near infrared spectroscopy (NIRS): background and current applications. *J Clin Monit Comput*.

2012;26(4):279-287. doi:10.1007/s10877-012-9348-y
20. Lu H, Xu F, Grgac K, Liu P, Qin Q, van Zijl P. Calibration and validation of TRUST MRI for the estimation of cerebral blood oxygenation. *Magn Reson Med*. 2012;67(1):42-49. doi:10.1002/mrm.22970
21. Enzmann DR, Ross MR, Marks MP, Pelc NJ. Blood flow in major cerebral arteries measured by phase-contrast cine MR. *AJNR Am J Neuroradiol*. 1994;15(1):123-129. http://www.ncbi.nlm.nih.gov/pubmed/8141043. Accessed August 18, 2019.
22. Bush AM, Coates TD, Wood JC. Diminished cerebral oxygen extraction and metabolic rate in sickle cell disease using T2 relaxation under spin tagging MRI. *Magn Reson Med*. 2018;80(1):294-303. doi:10.1002/mrm.27015
23. Coloigner J, Kim Y, Bush A, et al. Contrasting resting-state fMRI abnormalities from sickle and non-sickle anemia. Kassner A, ed. *PLoS One*. 2017;12(10):e0184860. doi:10.1371/journal.pone.0184860
24. DeBaun MR, Gordon M, McKinstry RC, et al. Controlled Trial of Transfusions for Silent Cerebral Infarcts in Sickle Cell Anemia. *N Engl J Med*. 2014;371(8):699-710. doi:10.1056/NEJMoa1401731
25. Grabner G, Janke AL, Budge MM, Smith D, Pruessner J, Collins DL. Symmetric atlasing and model based segmentation: an application to the hippocampus in older adults. *Med Image Comput Comput Assist Interv*. 2006;9(Pt 2):58-66. http://www.ncbi.nlm.nih.gov/pubmed/17354756. Accessed May 6, 2019.
26. Tatu L, Moulin T, Vuillier F, Bogousslavsky J. Arterial Territories of the Human Brain. In: *Frontiers of Neurology and Neuroscience*. Vol 30. ; 2012:99-110. doi:10.1159/000333602
27. Bush A, Chai Y, Choi SY, et al. Pseudo Continuous Arterial Spin Labeling Quantification in Anemic Subjects with Hyperemic Cerebral Blood Flow. *Magn Reson Imaging*. 2018;47:137. doi:10.1016/J.MRI.2017.12.011
28. Bush A, Borzage M, Detterich J, et al. Empirical model of human blood transverse relaxation at 3 T improves MRI T $_2$ oximetry. *Magn Reson Med*. 2017;77(6):2364-2371. doi:10.1002/mrm.26311
29. Bush A, Vu C, Choi S, et al. Calibration of T2 oximetry MRI for subjects with sickle cell disease. *Magn Reson Med*. 2021;86(2):1019-1028. doi:10.1002/mrm.28757
30. Reinhart K, Bloos F, Konig F, Bredle D, Hannemann L. Reversible decrease of oxygen consumption by hyperoxia. *Chest*. 1991;99(3):690-694. doi:10.1378/chest.99.3.690
31. Cox RW. AFNI: software for analysis and visualization of functional magnetic resonance neuroimages. *Comput Biomed Res*. 1996;29(3):162-173. http://www.ncbi.nlm.nih.gov/pubmed/8812068. Accessed May 18, 2018.
32. Ford AL, Ragan DK, Fellah S, et al. Silent infarcts in sickle cell disease occur in the border zone region and are associated with low cerebral blood flow. *Blood*. 2018;132(16):1714-1723. doi:10.1182/blood-2018-04-841247
33. Shen J, Miao X, Vu C, et al. Anemia Increases Oxygen Extraction Fraction in Deep Brain Structures but Not in the Cerebral Cortex. *Front Physiol*. 2022;13:896006. doi:10.3389/fphys.2022.896006
34. Guilliams KP, Fields ME, Ragan DK, et al. Large-Vessel Vasculopathy in Children With Sickle Cell Disease: A Magnetic Resonance Imaging Study of Infarct Topography and Focal Atrophy. *Pediatr Neurol*. 2017;69:49-57. doi:10.1016/j.pediatrneurol.2016.11.005
35. Losert C, Peller M, Schneider P, Reiser M. Oxygen-enhanced MRI of the brain. *Magn Reson Med*. 2002;48(2):271-277. doi:10.1002/mrm.10215
36. Hlatky R, Valadka AB, Gopinath SP, Robertson CS. Brain Tissue Oxygen Tension Response to Induced Hyperoxia Reduced in Hypoperfused Brain. *J Neurosurg*. 2008;108(1):53-58. doi:10.3171/JNS/2008/108/01/0053
37. Huppert TJ, Hoge RD, Diamond SG, Franceschini MA, Boas DA. A temporal comparison of BOLD, ASL, and NIRS hemodynamic responses to motor stimuli in adult humans.

Neuroimage. 2006;29(2):368-382. doi:10.1016/j.neuroimage.2005.08.065
38. Coloigner J, Vu C, Borzage M, et al. Transient Hypoxia Model Revealed Cerebrovascular Impairment in Anemia Using BOLD MRI and Near-Infrared Spectroscopy. *J Magn Reson Imaging*. July 2020:jmri.27210. doi:10.1002/jmri.27210
39. Chiarelli PA, Bulte DP, Wise R, Gallichan D, Jezzard P. A calibration method for quantitative BOLD fMRI based on hyperoxia. *Neuroimage*. 2007;37(3):808-820. doi:10.1016/J.NEUROIMAGE.2007.05.033
40. Watson NA, Beards SC, Altaf N, Kassner A, Jackson A. The effect of hyperoxia on cerebral blood flow: A study in healthy volunteers using magnetic resonance phase-contrast angiography. *Eur J Anaesthesiol*. 2000;17(3):152-159. doi:10.1046/j.1365-2346.2000.00640.x
41. Floyd TF, Clark JM, Gelfand R, et al. Independent cerebral vasoconstrictive effects of hyperoxia and accompanying arterial hypocapnia at 1 ATA. *J Appl Physiol*. 2003;95(6):2453-2461. doi:10.1152/japplphysiol.00303.2003
42. Mouren S, Souktani R, Beaussier M, et al. Mechanisms of coronary vasoconstriction induced by high arterial oxygen tension. *Am J Physiol Circ Physiol*. 1997;272(1):H67-H75. doi:10.1152/ajpheart.1997.272.1.H67
43. Demchenko IT, Boso AE, Bennett PB, Whorton AR, Piantadosi CA. Hyperbaric oxygen reduces cerebral blood flow by inactivating nitric oxide. *Nitric Oxide - Biol Chem*. 2000;4(6):597-608. doi:10.1006/niox.2000.0313
44. Karetzky MS, Keighley JF, Mithoefer JC. The effect of oxygen administration on gas exchange and cardiopulmonary function in normal subjects. *Respir Physiol*. 1971;12(3):361-370. doi:10.1016/0034-5687(71)90076-4
45. Smit B, Smulders YM, Eringa EC, et al. Hyperoxia does not affect oxygen delivery in healthy volunteers while causing a decrease in sublingual perfusion. *Microcirculation*. 2018;25(2). doi:10.1111/micc.12433
46. Bodetoft S, Carlsson M, Arheden H, Ekelund U. Effects of oxygen inhalation on cardiac output, coronary blood flow and oxygen delivery in healthy individuals, assessed with MRI. *Eur J Emerg Med*. 2011;18(1):25-30. doi:10.1097/MEJ.0b013e32833a295e
47. Lauscher P, Lauscher S, Kertscho H, Habler O, Meier J. Hyperoxia Reversibly Alters Oxygen Consumption and Metabolism. *Sci World J*. 2012;2012. doi:10.1100/2012/410321
48. Xu F, Liu P, Pascual JM, Xiao G, Lu H. Effect of hypoxia and hyperoxia on cerebral blood flow, blood oxygenation, and oxidative metabolism. *J Cereb Blood Flow Metab*. 2012;32(10):1909-1918. doi:10.1038/jcbfm.2012.93
49. Vu C, Bush A, Choi S, et al. Reduced global cerebral oxygen metabolic rate in sickle cell disease and chronic anemias. *Am J Hematol*. 2021;96(8):901-913. doi:10.1002/AJH.26203
50. Wood JC. Red Cells, Iron, and Erythropoiesis: Brain O2 reserve in sickle cell disease. *Blood*. 2019;133(22):2356. doi:10.1182/BLOOD-2019-04-901124
51. Croal PL, Leung J, Phillips CL, Serafin MG, Kassner A. Quantification of pathophysiological alterations in venous oxygen saturation: A comparison of global MR susceptometry techniques. *Magn Reson Imaging*. 2019;58:18-23. doi:10.1016/j.mri.2019.01.008
52. Angleys H, Østergaard L, Jespersen SN. The effects of capillary transit time heterogeneity (CTH) on brain oxygenation. *J Cereb Blood Flow Metab*. 2015;35(5):806-817. doi:10.1038/JCBFM.2014.254
53. Juttukonda MR, Donahue MJ, Waddle SL, et al. Reduced oxygen extraction efficiency in sickle cell anemia patients with evidence of cerebral capillary shunting. *J Cereb Blood Flow Metab*. 2021;41(3):546-560. doi:10.1177/0271678X20913123
54. Chu DK, Kim LHY, Young PJ, et al. Mortality and morbidity in acutely ill adults treated with liberal versus conservative oxygen therapy (IOTA): a systematic review and meta-analysis. *Lancet*. 2018;391(10131):1693-1705. doi:10.1016/S0140-6736(18)30479-3
55. Iscoe S, Beasley R, Fisher JA. Supplementary oxygen for nonhypoxemic patients: O

2much of a good thing? *Crit Care*. 2011;15(3):305. doi:10.1186/cc10229
56. Kallet RH, Branson RD. Should oxygen therapy be tightly regulated to minimize hyperoxia in critically ill patients? *Respir Care*. 2016;61(6):801-817. doi:10.4187/respcare.04933
57. Vu C, Bush A, Choi S, et al. Reduced global cerebral oxygen metabolic rate in sickle cell disease and chronic anemias. *Am J Hematol*. April 2021:ajh.26203. doi:10.1002/ajh.26203